

# Implicit Reconstructions from Deformed Projections for CryoET

Vinith Kishore\*, Valentin Debarnot\*, and Ivan Dokmanić\*†

\* University of Basel.

† University of Illinois at Urbana-Champaign.

**Abstract**—Cryo-electron tomography (cryoET) is a technique that captures images of biological samples at different tilts, preserving their native state as much as possible. Along with the partial tilt series and noise, one of the major challenges in estimating the accurate 3D structure of the sample is the deformations in the images incurred during the acquisition. We model these deformations as continuous operators and estimate the unknown 3D volume using implicit neural representations. This framework allows to easily incorporate the deformation and estimate jointly the deformation parameters and the volume using a standard optimization algorithm. This approach doesn't require training data and can benefit from standard prior in the optimization procedure.

## I. INTRODUCTION

Cryo-Electron Tomography (cryoET) [1] is an emerging imaging modality used to image biological samples such as cells, tissue, etc. These samples are flash-frozen and imaged using an electron microscope. The process is very similar to cryo Electron Microscopy (cryoEM) which has gained much attention due to its ability to resolve larger bio-molecules on a nanometer scale. Unlike cryoEM, cryoET is used for larger scale samples, where we can almost capture the interaction between the components in situ. In cryoET multiple images of the sample are acquired by tilting the thin frozen sample along its axis, at a discrete set of tilt angles. Unlike cryoEM, we have a limited number of images to recover the complete information of the structure, this is known as the missing wedge in the Fourier domain, thus making the problem ill-posed. The tilt-series obtained from an unknown volume is defined as:

$$\mathbf{y}_m = \mathbf{P}(\mathbf{R}_{\theta_m}(\boldsymbol{\rho})) + \boldsymbol{\epsilon}_m \quad (1)$$

where  $\boldsymbol{\rho} \in \mathbb{R}^{N \times N \times N}$  is the volume density of the sample we are imaging. The 3D-rotation operator  $\mathbf{R}_{\theta}(\cdot)$  tilts the volume by an angle  $\theta$  around a fixed axis,  $\mathbf{P} : \mathbb{R}^{N \times N \times N} \mapsto \mathbb{R}^{N \times N}$  is the projection operator and  $\boldsymbol{\epsilon}$  is the Gaussian noise which accounts for the low dose electron beam. The tilt  $\theta_m$  can only vary between -70 and +70 degrees resulting in a *missing wedge* of measurements.

This model accounts for the image formation case in which there are no mechanical faults or the sample is not affected by the electron beam. However, this is hardly the case in many applications of cryoET. Accounting for these deformations is crucial to obtain a high resolution reconstruction [2] and can be taken into account by the following forward model:

$$\mathbf{y}_m = \mathbf{D}_m(\mathbf{P}(\mathbf{R}_{\theta_m}(\boldsymbol{\rho}))) + \boldsymbol{\epsilon}_m, \quad (2)$$

where  $\mathbf{D}_m$  models deformations appearing in cryoET. Deformations are composed of rigid deformations due to the sample slightly moving between tilts, and local and non-rigid deformations due to the electron beam interacting with the sample. In this paper, we consider independent deformations on the tilt-series.

### A. Related work

AreTomo [3] is one such approach where patches from images are tracked to account for and correct deformations. Such methods

that use patch-based tracking can be useful in many applications but cannot track small-scale deformations that can occur within the patch nor deformations that appear between patches. Our approach is similar to AreTomo with the difference that we track all pixels simultaneously.

Neural fields (or implicit neural networks) represent continuous signals as maps from coordinates to function values [4]. Such models have been used extensively in inverse rendering problems [5]. Nerfies [6] was proposed in this problem to capture the deformations that vary continuously between scenes. Lately, it has also been successfully applied to model the volume density in cryoEM [7, 8], obtaining accurate reconstructions even with strong structural heterogeneity and noise. This was extended to Scanning Transmission Electron Microscopy [9]. In this paper, we propose to model both the unknown volume and the unknown deformation using neural fields in cryoET. Contrary to [6], we capture deformations that change randomly between images of the tilt-series.

Recently, [10] showed that global deformations (shear, rotations, and shifts) in the images can be recovered by appropriately modeling them and estimating the deformation parameters. In this paper, we employ a similar approach but we model directly the unknown volume using an implicit neural network. We also consider a wider class of deformations.

### B. Contributions

We propose an unsupervised method to jointly reconstruct the volume and the deformation from noisy and deformed tilt-series in cryoET. We extend previous work [10] by considering a rich class of deformation that accurately model cryoET acquisitions. Moreover, our original framework allows a significant gain in computation time and resources, while offering the possibility to be paired with sophisticated priors in order to compensate for the missing wedge.

## II. METHODS

We approximate the volume  $\boldsymbol{\rho}$  by an implicit representation  $\mathbf{V}(\boldsymbol{\psi}) : \mathbb{R}^3 \rightarrow \mathbb{R}$ , parameterized by  $\boldsymbol{\psi}$ . We use an MLP (Multi-Layer Perceptron) with Fourier feature as positional encoding. Using an implicit representation of the volume allows fast computation of the formation model (1) using discretization. The same benefit holds for any deformation acting on the coordinate space.

We approximate the deformations  $\mathbf{D}_m$  as:

$$\mathbf{D}(\phi_m) \stackrel{\text{def.}}{=} \mathbf{L}_m(\boldsymbol{\gamma}_m) \mathbf{S}(\boldsymbol{\tau}_m) \mathbf{R}_{2D}(\alpha_m)$$

where  $\mathbf{R}_{2D}(\alpha)$  is a 2D rotation operator by angle  $\alpha$ ,  $\mathbf{S}(\boldsymbol{\tau})$  is a shift operator with displacement  $\boldsymbol{\tau} = (\tau_x, \tau_y)$  and  $\mathbf{L}(\boldsymbol{\gamma}) : \mathbb{R}^2 \rightarrow \mathbb{R}^2$  is an implicit representation, parameterized by  $\boldsymbol{\gamma}$ , which models local deformations

$$(\mathbf{L}(\boldsymbol{\gamma})v)(\mathbf{x}) = v(\mathbf{x} + \mathbf{l}(\boldsymbol{\gamma})(\mathbf{x})), \forall v \in \mathcal{C}^0(\mathbb{R}^2), \forall \mathbf{x} \in \mathbb{R}^2,$$

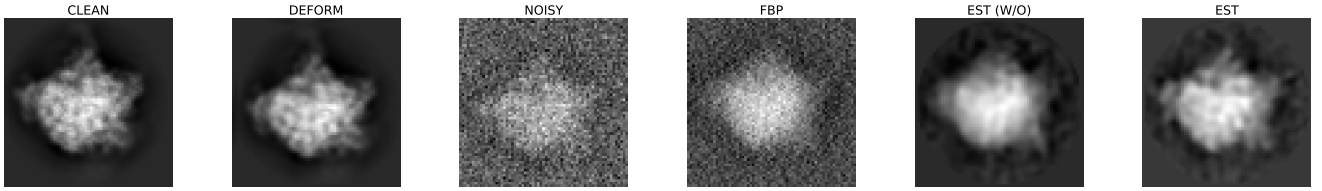


Fig. 1: Projections corresponding to the central viewing direction at angle 0 degree. From left to right, projection that is: non-deformed and noise-free, deformed and noise free, noisy and deformed (observation), estimated by the FBP, estimated while not accounting for the deformations (EST W/O), estimated with our method (EST).

where  $\mathbf{I}(\gamma) : \mathbb{R}^2 \rightarrow \mathbb{R}^2$  is a continuous operator in each of its output. To account for randomness in the local deformations, we use as many networks as there are images, as each network learns the local deformation of its image. The implicit representations  $\mathbf{L}_m$  could also be used to learn the inplane rootation and the shift operators, but we observe better performance when explicitly dissociate these three operators. Similar observation has already been made in Nerfies [6]. Unlike Nerfies, we use separate networks to capture local deformations from one image to the other, as we do not have continuous deformations between them. We learn the parameters  $\{\phi_m = (\gamma_m, \tau_m, \alpha_m)\}_{m=1}^M$  and  $\{\psi_m\}_{m=1}^M$  jointly by minimizing the mean square error between the observations and the estimated tilt-series:

$$\min_{\{\phi_m\}_{m=1}^M, \{\psi_m\}_{m=1}^M} \sum_{m=1}^M \|\mathbf{y}_m - \mathbf{D}(\phi_m)(\mathbf{P}(\mathbf{R}_{\theta_m}(\mathbf{V}(\psi_m))))\|_2^2 \quad (3)$$

Notice that the above formulation allows mini-batch optimization in the pixel space contrary to [10].

### III. EXPERIMENT AND RESULTS

We use the voxelized M. pneumoniae cell [11] (dataset DOI on EMPIAR 10.6019/EMPIAR-10499) model to test the recovery capacity of the model when there are deformations present. We simulate the cryoET observation by projecting the volume after rotation along a fixed axis at  $M = 90$  angles uniformly spaced between  $-70$  degrees to  $70$  degrees. We define the signal to noise ratio (SNR) between two signals  $\mathbf{s}, \mathbf{s}_{\text{true}} \in \mathbb{R}^N$  as

$$\text{SNR}(\mathbf{s}, \mathbf{s}_{\text{true}}) = 10 \log_{10} \left( \frac{\text{Var}(\mathbf{s})}{\text{Var}(\mathbf{s}_{\text{true}})} \right).$$

We add Gaussian noise so that the noisy projections have an SNR of 0dB. In the simulations, the true unknown deformations  $\mathbf{D}_m$  are the composition of a smooth random diffeomorphism as defined in [12], a random shift with maximum  $\pm 10\%$  of the image size, and a random in-plane rotation with angle between  $\pm 10$  degrees.

In the following, we compare our approach that involves estimating deformations (EST) with our approach where we simply fit an implicit neural network to estimate the volume but without accounting for the deformation (EST W/O). We also compare with the filtered-back projection (FBP) [13], a standard reconstruction algorithm.

We display a snapshot of the true and estimated volumes in Figure 2. We asses the quality of the reconstruction using the Fourier Shell correlation (FSC) in Figure 3. The FSC indicates the correlation between the frequencies of the estimated volume and the original. This is a standard metric used to compare recovered volumes in practice [13]. Figure 3 shows that estimating the deformation allows a significant increase in the resolution. Notice that all three methods don't compensate for the missing wedge, and we expect a higher gain when incorporating additional prior in Problem (3).

	EST	EST (W/O)	FBP
Shifts (pixel)	0.7396	3.3863	3.3863
In-plane rotation (degree)	1.5837	5.067	5.067
local deformation (pixel)	1.284	1.282	1.282
SNR of projections (dB)	14.962	11.999	-6.873

TABLE I: Estimation quality of the parameters at SNR 0dB.

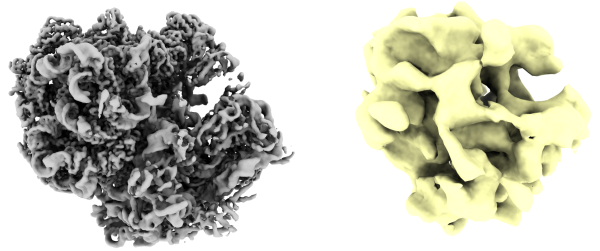


Fig. 2: Snapshot of the true (left) and estimated (right) volume.

We asses the quality of the estimation of deformation in Table I. We display the average error on the global deformations (shift and in-plane rotation). We also report the average SNR of the noise-free and non-deformed projections between the true and estimated volume. While the deformation parameters are well estimated, the gain of SNR in the projections also indicates that the volume is better estimated than when no deformation is estimated.

### IV. CONCLUSION

We show that pixel-level deformations, widely present in many cryoET applications, can be mitigated using a small set of parameters and networks. Along with this, we use an implicit network to represent the undistorted volume and jointly learn to recover it even in the presence of unknown deformations. We see improvements in the reconstructions. The current setup relies on the inductive bias of the implicit network to accurately recover volume. However, our framework is flexible enough to allow the use of advanced prior, helping to compensate for the missing wedge.

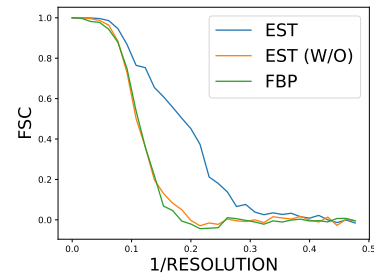


Fig. 3: FSC between three different estimations and the true volume.

## REFERENCES

- [1] A. Doerr, “Cryo-electron tomography,” *Nature Methods*, vol. 14, no. 1, pp. 34–34, 2017.
- [2] D. N. Mastronarde, “Fiducial marker and hybrid alignment methods for single-and double-axis tomography,” *Electron tomography: methods for three-dimensional visualization of structures in the cell*, pp. 163–185, 2006.
- [3] S. Zheng, G. Wolff, G. Greenan, Z. Chen, F. G. Faas, M. Bárcena, A. J. Koster, Y. Cheng, and D. A. Agard, “Aretomo: An integrated software package for automated marker-free, motion-corrected cryo-electron tomographic alignment and reconstruction,” *Journal of Structural Biology: X*, vol. 6, p. 100068, 2022.
- [4] B. Mildenhall, P. P. Srinivasan, M. Tancik, J. T. Barron, R. Ramamoorthi, and R. Ng, “Nerf: Representing scenes as neural radiance fields for view synthesis,” *Communications of the ACM*, vol. 65, no. 1, pp. 99–106, 2021.
- [5] V. Sitzmann, J. Martel, A. Bergman, D. Lindell, and G. Wetzstein, “Implicit neural representations with periodic activation functions,” *Advances in Neural Information Processing Systems*, vol. 33, pp. 7462–7473, 2020.
- [6] K. Park, U. Sinha, J. T. Barron, S. Bouaziz, D. B. Goldman, S. M. Seitz, and R. Martin-Brualla, “Nerfies: Deformable neural radiance fields,” in *Proceedings of the IEEE/CVF International Conference on Computer Vision*, 2021, pp. 5865–5874.
- [7] E. D. Zhong, T. Bepler, B. Berger, and J. H. Davis, “Cryodrgn: reconstruction of heterogeneous cryo-em structures using neural networks,” *Nature methods*, vol. 18, no. 2, pp. 176–185, 2021.
- [8] A. Levy, F. Poitevin, J. Martel, Y. Nashed, A. Peck, N. Miolane, D. Ratner, M. Dunne, and G. Wetzstein, “Cryoai: Amortized inference of poses for ab initio reconstruction of 3d molecular volumes from real cryo-em images,” in *Computer Vision—ECCV 2022: 17th European Conference, Tel Aviv, Israel, October 23–27, 2022, Proceedings, Part XXI*. Springer, 2022, pp. 540–557.
- [9] H. Kniesel, T. Ropinski, T. Bergner, K. S. Devan, C. Read, P. Walther, T. Ritschel, and P. Hermosilla, “Clean implicit 3d structure from noisy 2d stem images,” in *Proceedings of the IEEE/CVF Conference on Computer Vision and Pattern Recognition*, 2022, pp. 20 762–20 772.
- [10] V. Debarnot, S. Gupta, K. Kothari, and I. Dokmanic, “Joint cryo-et alignment and reconstruction with neural deformation fields,” *arXiv preprint arXiv:2211.14534*, 2022.
- [11] D. Tegunov, L. Xue, C. Dienemann, P. Cramer, and J. Mahamid, “Multi-particle cryo-em refinement with m visualizes ribosome-antibiotic complex at 3.5 Å in cells,” *Nature Methods*, vol. 18, no. 2, pp. 186–193, 2021.
- [12] O. Ronneberger, P. Fischer, and T. Brox, “U-net: Convolutional networks for biomedical image segmentation,” in *Medical Image Computing and Computer-Assisted Intervention—MICCAI 2015: 18th International Conference, Munich, Germany, October 5–9, 2015, Proceedings, Part III 18*. Springer, 2015, pp. 234–241.
- [13] G. Harauz and M. van Heel, “Exact filters for general geometry three dimensional reconstruction.” *Optik.*, vol. 73, no. 4, pp. 146–156, 1986.